Effects of rainfall-runoff pollution on eutrophication in coastal zone: a case study in Shenzhen Bay, southern China

Hongliang Xu, Ying Zhang, Xiuzhen Zhu and Mingfeng Zheng

ABSTRACT

The concentration of human activities in coastal cities results in the increase of nutrient salts released into the coastal environment and is identified as a major environmental problem for coastal zone management. Large amounts of nitrogen and phosphorus are transported by rainwater-runoff from urban catchments to coastal zones during episodic rainfall events inducing eutrophication problems and increasing the risk of red tide occurrence. This study used a coupled model based on the Storm Water Management Model (SWMM) and Environment Fluid Dynamic Code (EFDC) to simulate the rainfall-runoff pollution load and its effects on eutrophication in Shenzhen Bay, southern China. A storm event of 2014 was used to build the modeling scenarios and thus analyzed the spatial-temporal variation of the rainfall-runoff pollution. The results indicated that: (i) rainfall-runoff pollution loads accounted for 60–80% of the total pollution loads, and rainfall-runoff pollution can result in a short-term impact pollution load on the receiving seawater body; (ii) the transportation of nutrient salts in the coastal zone and the nutrient salts absorbing process by algae are at different times, which suggests urban rainfall-runoff pollution has evidently an effect on variation of the concentration of chlorophyll-A in the bay, and with increasing distance to the city, the seawater body is gradually less affected by rainfall-runoff pollution.

Key words | coupled model, EFDC, eutrophication, pollution, rainfall-runoff pollution, Shenzhen Bay, SWMM

Hongliang Xu (corresponding author)
School of Geographic and Oceanographic Sciences,
Nanjing University,
Nanjing 210023, Jiangsu,
China
and
Power China Water Environment Governance,
Shenzhen 518012, Guangdong,
China
E-mail: *hongliangxu.pku@outlook.com*

Ying Zhang
School of Urban Construction and Environmental Engineering,
Chongqing University,
Shapingba, Chongqing 400044,
China

Xiuzhen Zhu
Department of Chemistry,
Southern University of Science and Technology,
Shenzhen, 518055, Guangdong,
China

Hongliang Xu
Mingfeng Zheng
School of Environment and Energy,
Peking University Shenzhen Graduate School,
Shenzhen 518055, Guangdong,
China

INTRODUCTION

Rapid urbanization in coastal zones can result in increased emissions of nutrients, such as phosphorus (P) and nitrogen (N), into the surrounding environment. Pollutants (mainly N and P) in urban areas can be washed away by storm runoff, flow into natural water bodies and, ultimately, cause the eutrophication of lakes, rivers, and coastal waters, and meanwhile are a threat to ecosystem security.

Urban storm runoff is the main driving force for the migration and conversion of nutrients in urban areas (Brinkmann 1985). Nutrients, especially those containing N and P, exist widely in the natural environment. Moreover, industrial and agricultural activities also emit a large amount of nutrient salts into the surrounding environment (in which the nutrient salts released into the atmosphere play an important role in the formation of aerosols) and cause pollution. The nutrient salts accumulate in soil and water bodies and on the rough earth surface via pollutant emission and atmospheric dry deposition, etc., during non-rainy days. During rainfall events, aerosol particles get into cloud droplets through working as cloud nuclei, then the falling rain droplet particles collide with aerosol particles through Brownian diffusion, interception, impaction, and turbulent diffusion (Seinfeld *et al.* 1998). Finally, the nutrient salts are discharged into the surrounding

doi: 10.2166/nh.2019.012

coastal environment by leaching and wash off via surface flow and sewage system.

In urban areas, the surface runoff is generated and polluted on the ground and then flows into the municipal drainage system during rainfall events, and is finally discharged into natural waterbodies. Many studies have focused on the investigation of the formation and characteristics of nutrient loads on various surfaces, such as roofs and roads, in urban areas (Carpenter *et al.* 1998; Gnecco *et al.* 2005; Hathaway *et al.* 2012). Studies on the re-mobilization of sediments in stream and river channels have indicated that the initial scouring effect plays an important role in the formation of polluted surface runoff (Bertrand-Krajewski *et al.* 1998). To quantify the impact of polluted urban surface runoff on waterbodies, many empirical or conceptual process models (e.g., SWMM (Storm Water Management Model) and HSPF (Hydrological Simulation Program-Fortran)) have been developed to simulate the wash-off process of accumulated pollutants, and the transport and conversion processes of the polluted runoff in municipal sewage systems and in river channels. Burian *et al.* (2001) investigated the suitability of integrating deterministic models to estimate the relative contributions of atmospheric dry and wet deposition onto an urban surface and the subsequent volumes removed by stormwater runoff. Bergman *et al.* (2002) modeled pollutant loads during storm events in the South Prong watershed, USA, using HSPF and found that the prediction error of TSS (total suspended solids) and TP (total phosphorus) was 3% and 24%, respectively. Temprano *et al.* (2006) studied pollution fluxes during rainy weather in a combined sewer system catchment in Santander, Spain, using SWMM, and indicated that the accuracy of the total simulated loads of SS (suspended solids), COD (chemical oxygen demand) and TKN (total Kjeldahl nitrogen) at the end of the rainfall events were 93%, 95%, and 78%, respectively. Moreover, the loads emitted during the first-flush events were determined to account for 65%, 57%, and 54% of the total polluting loads of COD, SS, and TKN, respectively.

In coastal cities, pollutants in storm runoff will eventually be transported into the natural waterbodies such as sea, rivers, and lakes, and will result in the deterioration of water quality (Josefson & Rasmussen 2000; Kemp *et al.* 2005; Bricker *et al.* 2008; Chen *et al.* 2017). Storm runoff contains many kinds of pollutants (e.g., N, P, heavy metals, petroleum hydrocarbons, etc.). The increase of nutrient concentrations (mainly N and P) which are caused by the polluted surface runoff can easily lead to a red tide breakout under appropriate weather and environmental conditions (Villarino *et al.* 1995; Conley *et al.* 2009). It should be noted that storm runoff not only conveys nutrient salts to the coastal waters, but also contains toxic pollutants (e.g., heavy metals, organo-chlorine pesticide, polycyclic aromatic hydrocarbons, etc.) that can inhibit algal growth but are low in concentrations. After the dilution by coastal waters, the toxic pollutants in urban storm runoff pose an even more subtle influence on inhibiting algal growth. Turner & Rabalais (2004) studied the annual loads of C, N, P, silicate, TSS and their yields in six watersheds of the Mississippi River Basin, USA, using water quality and water discharge records from 1973 to 1994. They found that the increase of inorganic nitrogen and bio-available phosphate resulted in algae blooms in the northern Gulf of Mexico. Bowes *et al.* (2005) investigated the seasonal variation of TP, PP (particulate phosphorus) and SRP (soluble reactive phosphorus) concentrations at three points along the River Swale in England, and pointed out that P from storm runoff was the dominant factor causing eutrophication in the intertidal zone of the river mouth. Maillard & Santos (2008) evaluated the effects of land use and land cover on the quality of nearby stream water in a semi-arid watershed in southeastern Brazil. The results suggested a strong relationship between land use and land cover on turbidity, along with higher concentrations of N and fecal coliforms. This demonstrated that storm runoff during the rainy season conveyed more organic material into the sea and led to the deterioration of seawater quality. Saniewska *et al.* (2018) investigated the impact of intense rains and flooding on the input of mercury into the coastal zone of the southern Baltic region and found that the decreased retention of mercury during intense rainfalls demonstrated mercury elution from the catchment. Meanwhile, floods, melting snow, and development of urban infrastructure and farmlands increases also have a tremendous impact on the outflow of mercury from the catchment. Rossi *et al.* (2018) investigated the space–time dynamics of N pollution in a Mediterranean gulf by means of $\delta^{15}N$ variation and found that coastal and offshore areas were vulnerable to

freshwater-transported nutrients, consistent with terrestrial hydromorphology and sea surface-water circulation.

In recent decades, many marine ecological dynamic models have been developed to simulate, predict, and manage the coastal zone environment. For example, USEPA (United States Environmental Protection Agency) recommends the use of WASP (Water Quality Analysis Simulation Program) and MIKE (developed by DHI (Dansk Hydraulisk Institut)) to model the variation of water quality in coastal zones. The models have been successfully applied to simulate the eutrophication of estuary water bodies in many areas, such as Chesapeake Bay (Hamrick & Wu 1997) and the river mouth of the Neuse River (Wool *et al.* 2003) in the USA, Kwang-Yang Bay, South Korea (Park *et al.* 2005), Narva Bay, Estonia (Lessin & Raudsepp 2007), the Perth coastal margin, south-western Australia (Machado & Imberger 2014), Virginia Beach (Johnson & Sample 2017), etc. With the help of these prediction models, many studies have indicated that storm runoff contributed 55% of the total pollutant loads in coastal zones in the USA and investigations in Europe have also provided similar conclusions (Goonetilleke *et al.* 2005).

Based on the foregoing studies, it is evident that many investigations took into account storm runoff pollution in coastal urban areas using various methods. The formation mechanisms of storm runoff pollution and their characteristics have been studied extensively. Meanwhile, many computer models based on hydrological, physical, and chemical processes are being developed to analyze the spatial-temporal variation of pollutant outputs at basin scale. Furthermore, studies on eutrophication in coastal zones have mainly focused on the variation of the flux of nutrients, their transport and conversion mechanisms, and the relationship between algal growth and environmental factors. However, the effect of nutrients (mainly N and P) carried by the storm-generated surface runoff on the variation of eutrophication (reflected by the concentration of chlorophyll-A) in coastal zones has not yet been the subject of much research attention, and the spatial and temporal variation of algae proliferation after a single storm event in offshore areas remains unclear. The above considerations form the basis of this study, and the objectives of this study were to: (1) study the spatial-temporal variation of nutrient salts in an offshore area under storm runoff pollution; and (2) assess the use of coupled simulation and prediction models in chain on analyzing the variation of algae blooms that respond to the nutrient salts from urban storm runoff to coastal recipient.

STUDY AREA AND DATA

Study area

The Shenzhen Bay Basin is located at 22.36°–22.61°N and 113.87°–114.18°E, in the eastern Pearl River Delta, southern China (Figure 1). Shenzhen Bay is a semi-closed gulf, and the basin covers a 607 km^2 land area in Shenzhen and Hong Kong, while the bay itself is a 15 km long and 5.5 km wide semi-closed bay of 83 km^2 and mean depth of 3 m. Mountains and hills are distributed along the north of the basin and are the sources of the rivers flowing into the bay. The basin is dominated by a subtropical maritime monsoon climate with an annual mean temperature of 22.4 °C and a multi-year mean precipitation of 1,883 mm. The rainy season is from April to September and accounts for approximately 80% of the annual rainfall. The terrain in the basin results in floods that have a short confluence time and a high peak runoff volume during rainy season storms. The basin is highly urbanized with a population of nearly 3.5 million. Due to the lack of effective regulation, a large amount of wastewater from industrial activities without treatment pollutes the rivers and leads to a large amount of terrigenous pollutants (including nutrients, petroleum hydrocarbon, heavy metals, etc.) being emitted into the bay.

Data

Nutrient salts and chlorophyll-A concentrations, which were monitored online in 2014 from eight buoys in Shenzhen Bay (Figure 1), were used to analyze the variation of the seawater quality in the bay.

The surface runoff pollution data were monitored on April 5th 2012 and April 16th 2014, respectively. The concentrations of nitrate (NO_3-N), ammonia nitrogen (NH_3-N), and phosphate (PO_4^{3-}) in the surface runoff originating from typical industrial land, residential land, and roads were tested under different periods of the storm events.

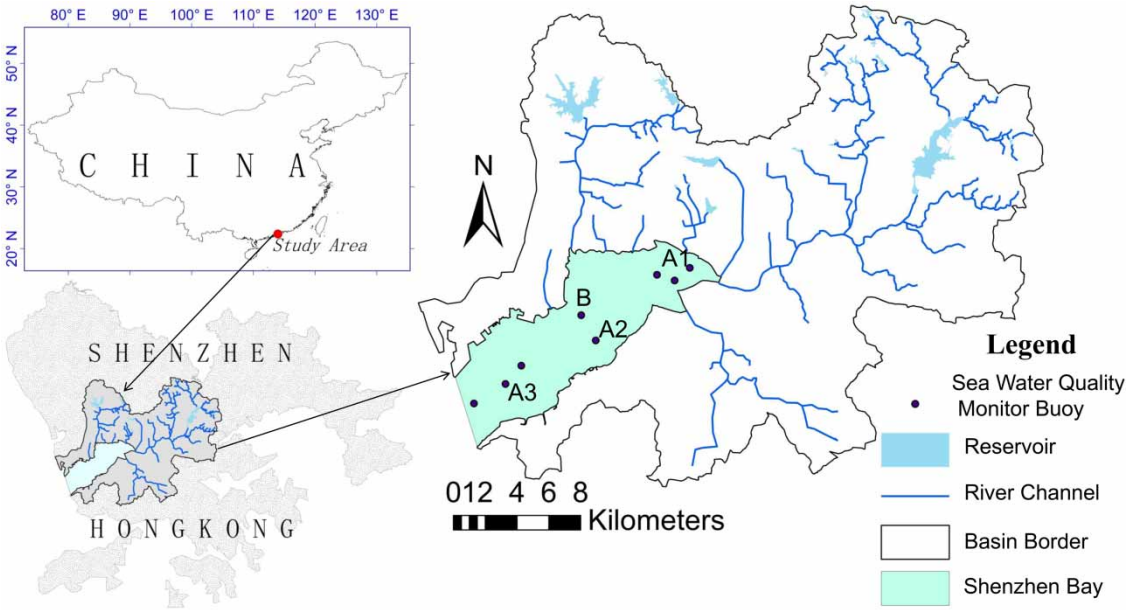

Figure 1 | Study area: Shenzhen Bay Basin.

The land-use map includes five kinds of land-use types: industrial land, residential land, road, water body, and green landscapes. It was derived from Landsat TM images by using supervised classification method in ENVI, 90 m resolution digital elevation model (DEM) of Shenzhen Bay Basin, municipal sewage system map, weather data, monitored surface runoff pollution data, point-source pollution data, river water quality data, seawater quality data, tide level, and seabed elevation, which were used as input of SWMM and EFDC (Environment Fluid Dynamic Code), and modeled the variation of pollutant loads in the rivers and in the bay during storm events.

METHODOLOGY

Environmental models

As the migration and conversion of the nutrient salts in storm runoff relate to both the land and sea areas, significant interactions between sea and land can be observed. To analyze the effects of storm runoff pollution in coastal urban areas on the coastal water environment, this study made use of two models, SWMM and EFDC, to simulate storm runoff pollution and eutrophication in Shenzhen Bay, respectively.

USEPA's SWMM is a widely used computer model that accounts for various hydrologic processes that produce runoff from urban areas and estimates the production of pollutant loads associated with stormwater runoff (Chang *et al.* 2015; Guan *et al.* 2015; Shuster *et al.* 2015; Estalaki *et al.* 2016). It is a dynamic hydrologic–hydraulic water quality simulation model that can be used for single events or for long-term (continuous) simulation of runoff quantity and quality from primarily urban areas. The runoff component operates on a collection of sub-catchment areas that receive precipitation, and generate runoff and pollutant loads. The routing portion transports this runoff through a system of pipes, channels, storage/treatment facilities, pumps, and flow regulators. The quantity and quality of runoff modeled in SWMM is generated within each sub-catchment. The model tracks the flow rate, flow depth, and quality of water in each pipe, and then channels it during a simulation period made up of multiple time steps.

EFDC is a state-of-the-art multi-functional surface water modeling system developed by USEPA that can be used to simulate aquatic and coastal systems in one, two, and three dimensions. The model includes hydrodynamic, sediment-contaminant, and eutrophication components. It has been successfully applied in the modeling of environmental changes in water bodies (e.g., rivers, lakes, reservoirs, wetlands, estuaries,

and coastal ocean regions) to support environmental assessment and management (Liu *et al.* 2008; O'Donncha *et al.* 2013; Chen *et al.* 2016). The computational scheme of the model utilizes an external–internal mode splitting, used to solve horizontal momentum equations and the continuity equation on a staggered grid. The transport equations for turbulence intensity, turbulence length scale, salinity, temperature, suspended sediments, dissolved and adsorbed contaminants, and dye tracer are also solved, using a fractional step scheme with implicit vertical diffusion and explicit advection and horizontal diffusion (EFDC User Manual 2007).

Process of modeling eutrophication

This study made use of the output of SWMM as the input of EFDC to model the impact of storm runoff pollution on the coastal zone. First, the study area was divided into two subsystems, i.e., the urban area and the offshore area. The polluted storm runoff was produced in the urban area, and the offshore area received the polluted runoff and provided the growth environment of algae. The collected data (regarding the river network, municipal sewage system, point source pollution, rainfall, tide level, salinity, water quality, solar radiation, etc.) were analyzed and the key interaction processes that effect eutrophication between the urban and offshore area were identified. Finally, the SWMM and EFDC models were calibrated and then applied in various scenarios to analyze eutrophication in Shenzhen Bay during and after storm events.

Calibration and validation of SWMM and EFDC

SWMM was calibrated based on monitored storm runoff pollution data and meteorological data. Meanwhile, the model used four parameters (Table 1) to simulate the water quality indices (NO_3-N, NH_3-N, and PO_4^{3-}) in three different land surfaces (i.e., road, industrial land, and residential land).

The validated *NSE* (Nash–Sutcliffe model efficiency coefficient) values were 0.65–0.88, indicating that the SWMM was suitable for the simulation of storm runoff pollution in the urban area in this study. Figure 2 shows an example of the variation of the validated pollution load under a storm event on three kinds of pavements (the black lines represent the simulated values while the hollow dots represent the concentration values of the nutrient salts in water samples collected from the curbside storm drains during storm events). It can be seen that SWMM can satisfactorily model the nutrient salts accumulated on the industrial land and the residential land in the urban area in the basin, while the simulation of the accumulated NH_3-N and PO_4^{3-} on the road produces relatively large errors, especially the monitored values of PO_4^{3-} concentration appear to be dispersed in the figure and not concentrated along the modeled curve (Figure 2(a2) and 2(a3)). It should be noted that different land surfaces host different human activities which result in different pollutant accumulation, e.g., high values of NO_3-N concentration (maximum 5.26 mg/L) was monitored on road surfaces due to a large amount of automobile exhaust emitted towards the road (Figure 2(a1)); high values of NO_3-N and NH_3-N concentration (maximum 5.04 mg/L and 5.06 mg/L, respectively) were monitored due to the sampling sites of industrial land located in a chemical industry park (Figure 2(b1) and 2(b2)); The monitoring sites of residential land were located near several restaurants which occupied parts of the sidewalk to run their business. Therefore, the pavement was polluted by the kitchen waste

Table 1 | The parameter values calibrated in SWMM

	Parameter[a]			
Landuse type	**c_1**	**c_2**	**c_3**	**c_4**
Residential land	0.32/0.22/0.08[b]	3/3/3	0.27/0.15/0.22	1.13/1.2/1.22
Industrial land	0.32/0.15/0.08	3/3/3	0.24/0.24/0.25	1.13/1.12/1.2
Road	0.22/0.24/0.11	3/3/3	0.12/0.07/0.08	1.13/1.2/1.22

[a]c_1 is maximum cumulant; c_2 is subsaturation cumulative time; c_3 is coefficient of scouring; c_4 is wash off index.
[b]0.32/0.22/0.08 represents the parameter values in modeling NH_3-N/NO_3-N/PO_4^{3-}.

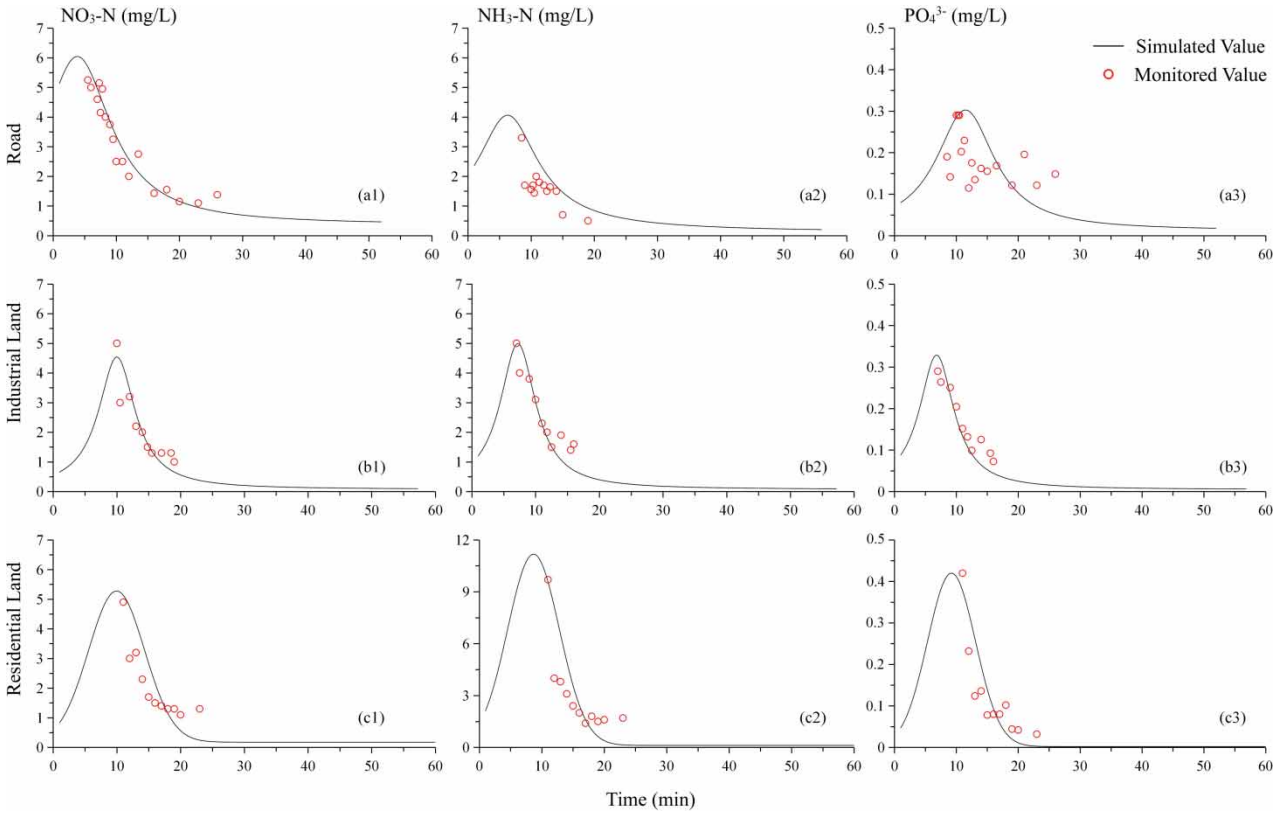

Figure 2 | The simulated nutrient salts on roads, industrial land, and residential land in SWMM.

and higher values of NH_3-N and PO_4^{3-} concentration (maximum 9.67 mg/L and 0.43 mg/L, respectively) were detected in residential land (Figure 2(c2) and 2(c3)).

However, for the study area located in the highly industrialized Pearl River Delta, sulfate (S), NO_3-N, and NH_3-N are the major water-soluble ions in particulate matter in the atmosphere (Dai *et al.* 2013). The particulate matter accumulates on the pavements via dry deposition, resulting in the concentration values of NO_3-N and NH_3-N in storm runoff from different land use not to appear obviously different.

Hydrodynamics and salinity play important roles in affecting the migration and diffusion of pollutants from urban storm runoff into estuaries. Accurate simulation of the hydrodynamic conditions and salinity is the basis of modeling the eutrophication in the bay. Monitored seawater quality data from 6th–15th in June and 16th–23rd in April, 2014 were used to calibrate and validate the EFDC model, respectively. In addition, 15 parameters were calibrated (Table 2) in the model after sensitive analysis to simulate the variation of the water quality in the bay.

Table 3 shows the statistical indices during EFDC's validation period. It can be seen that EFDC presented the smallest relative error (*RE*) ($RE = 0.02$) when modeling PO_4^{3-}, while the largest deviation appears when modeling salinity ($RE = 2.24$). The *NSE* values are all larger than 0.6, which indicates that the EFDC can satisfactorily reflect the dynamic variation of the modeled seawater quality data as compared to the monitored data.

RESULTS AND DISCUSSION

Variation of the water quality in Shenzhen Bay before and after rainfall

The monitored nutrient salts data during the wet and dry seasons of 2014 (Figure 3) in Shenzhen Bay indicated

Table 2 | The parameter values calibrated in EFDC

Parameter	Parameter meaning	Value	Unit
K_2	The coefficient of aeration	0.36	/
I_0	The optimum illumination intensity for algae growth	280	Langley/d
KHN	The half-saturation constant of the nitrogen absorption for algae growth	0.28	mg/L
KHP	The half-saturation constant of the phosphate absorption for algae growth	0.08	mg/L
PM	The algae growth rate	1.85	d^{-1}
BM	The algae metabolic rate	0.055	d^{-1}
PRR	The prey rate of algae	0.12	d^{-1}
WS	The deposition rate of algae	0.08	d^{-1}
RNITN	The maximum nitrification rate	0.056	$gN{\cdot}m^{-3}{\cdot}d^{-1}$
KDP	The minimum hydrolysis rate of DOP	0.12	d^{-1}
KLP	The minimum hydrolysis rate of LPOP	0.055	d^{-1}
KLN	The minimum hydrolysis rate of LPON	0.014	d^{-1}
KDN	The minimum hydrolysis rate of DON	0.056	d^{-1}
CChl	The ratio between carbon and chlorophyll	0.055	$mgC/\mu gChl$
ANC	The ratio between nitrogen and carbon	0.23	/

Table 3 | The validation results of the simulated hydrodynamic and seawater quality indices in Shenzhen Bay in EFDC

	RE	RMSE	NSE
Tide level	0.26	0.08	0.89
Salinity	2.24	1.29	0.74
NO_3-N	0.29	0.24	0.66
NH_3-N	0.05	0.05	0.61
PO_4^{3-}	0.02	0.01	0.77
Chlorophyll-A	0.2	0.27	0.83

that the nutrient salts' concentrations during the wet season were noticeably higher than those during the dry season. This was attributed to the fact that the sediments in the drainage pipes and river channels flowed into the bay, and

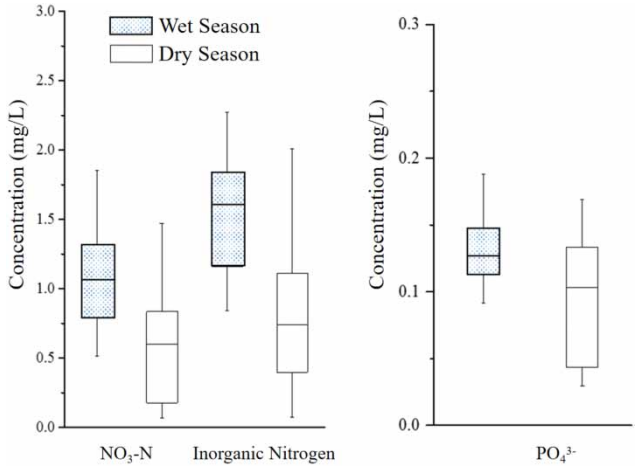

Figure 3 | The monitored nutrient salts in the wet season and dry season in 2014 in Shenzhen Bay.

together with the poor hydrodynamic conditions in the bay, resulted in the deterioration of the seawater quality. It can be seen that the concentrations of NO_3-N, inorganic nitrogen, and PO_4^{3-} were 0.51–1.83 mg/L, 0.78–2.23 mg/L, and 0.09–0.19 mg/L during the wet season, respectively, while they were 0.07–1.42 mg/L, 0.07–2.09 mg/L, and 0.03–0.17 mg/L during the dry season, respectively.

More specifically, the monitored inorganic nitrogen and PO_4^{3-} concentrations before and after four rain events in one buoy (point B in Figure 1) are presented in Table 4. It can be observed from the table that the rain volume, rain duration, and the duration of the antecedent dry period clearly impact the concentrations of N and P in the offshore seawater. The longer the antecedent dry period was, the larger were the pollutant loads accumulated on the urban ground surface that can then be washed off and transported into the sea. The pollutants were accumulated on rough surfaces and also concealed in the crevices of pavements, therefore, only a proportion of the cumulative pollutants can be washed off by surface flow; the higher the rain volume and the longer the rain duration were, the larger were the accumulated pollutant loads to be washed off. However, the relationships between the concentration of pollutants and the rain event characteristics are complex, and many factors (e.g., weather conditions and hydraulic conditions) may significantly affect the seawater quality after the pollutants have migrated into the sea.

Table 4 | The monitored inorganic nitrogen and PO_4^{3-} concentration before and after rain events in one buoy in Shenzhen Bay

				Peak values before rainfall (mg/L)		Peak values after rainfall (mg/L)	
Rain time	Rain amount (mm)	Duration (minutes)	Antecedent dry period (days)	Inorganic nitrogen	PO_4^{3-}	Inorganic nitrogen	PO_4^{3-}
2014/8/19	61.3	136	5	2.56	0.114	2.99	0.142
2014/9/6	28.4	70	4	2.61	0.120	2.88	0.135
2015/7/10	13.4	62	9	2.52	0.117	2.44	0.145
2015/9/21	157.4	153	8	2.53	0.123	3.10	0.158

Impacts of storm events on the eutrophication of Shenzhen Bay

Outputs of pollutant loads during storm events

A typical storm event of 72 mm accumulated rainfall with its antecedent dry period being longer than 5 days (occurring on March 30th, 2014, 2 hour duration and return period of one year) was selected to model the impact of storm runoff on the eutrophication in Shenzhen Bay. The simulation results suggested that the whole urban area in the basin output in total 14.54 tons of NH_3-N, 8.93 tons of NO_3-N, and 2.05 tons of PO_4^{3-}, respectively, into Shenzhen Bay due to the storm of March 30, 2014. In addition, we modeled the monthly output load of nutrient salts in storm runoff in 2014 by using SWMM (Figure 4). It is seen from Figure 4 that the rainfall in 2014 was mostly concentrated in the March to September period, and accompanied by the storms, the basin output most of the nutrient salts load during this period in the year. Most of the nutrient salts load was eventually transported into the bay and caused the deterioration of the bay water quality. From March to September, the output load of NH_3-N, NO_3-N, and PO_4^{3-} was 1,012.5 tons, 673.8 tons, and 87.6 tons in the storm runoff, respectively, which accounted for 87% of the annual total nutrient salts load (2,039 tons). It should be noted that river sediment is another important source of nutrient salts. In addition, the polluted muddy bottom layers of the rivers contain relatively high concentrations of N and P, and these can be released into waterbodies, particularly under flood conditions.

Furthermore, the simulated storm events (see Appendix, Table A1 and Figure A1, available with the online version of this paper), with different return periods were used to model

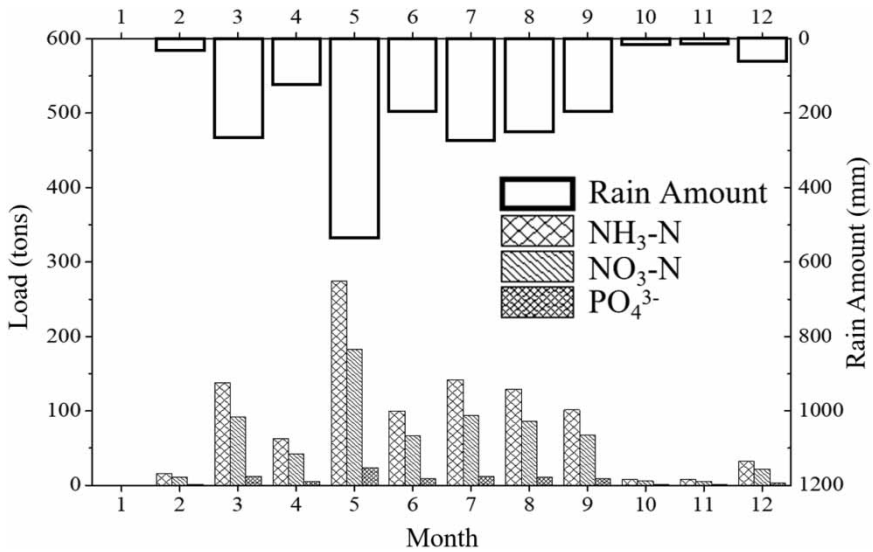

Figure 4 | The monthly rainfall amount and output load of nutrient salts in storm runoff in the study basin in 2014 modeled by SWMM.

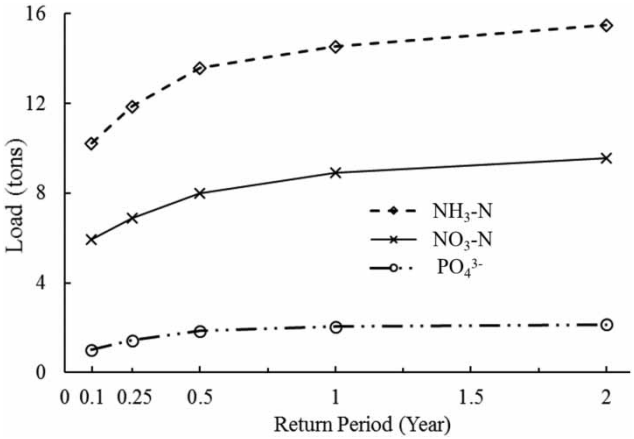

Figure 5 | The simulated load of nutrient salts under the storm events with different return periods.

the pollutant loads in storm runoff in the SWMM. It can be seen in Figure 5 that the loads of NO_3-N, PO_4^{3-}, and NH_3-N evidently increased with the increase of the return periods. The loads of NH_3-N, NO_3-N, and PO_4^{3-} increased rapidly from 10.22 tons, 5.92 tons, and 1.03 tons, respectively, to 13.58 tons, 8.01 tons, and 1.86 tons, respectively, when the return periods of the storm events increased from 0.1 year to 0.5 year. Meanwhile, the loads of the pollutants exhibited a slight increase when the return period was larger than 0.5 year.

Table 5 shows the proportion of the pollutant loads modeled for the designed storm runoff as part of the total pollutant loads that migrated into the sea. Under different designed storms, the pollutant loads produced by runoff were much larger than those produced by point-sources. The pollutant loads from runoff account for approximately 60–80% of the total pollutant loads during the concentration time and thus impacted the offshore receiving seawater quality obviously.

Table 5 | The proportion of modeled pollutant load from designed storm runoff in the total pollutant load (%)

		Return period (year)				
		0.1	0.25	0.5	1	2
Pollutant	NO_3-N	71.9	74.8	77.2	78.4	79.5
	NH_3-N	65.4	68.7	71.9	74.0	75.
	PO_4^{3-}	61.9	69.5	74.5	76.4	77.2

Impact of rainfall on the eutrophication in the bay using monitored data

The concentrations of NO_3-N, NH_3-N, PO_4^{3-}, and chlorophyll-A were monitored before and after the storm event that occurred on March 30th, 2014 in Shenzhen Bay. Figure 6 presents the distribution of the concentrations of nutrient salts and chlorophyll-A in the bay on the first day prior to the storm event (marked as −1d) and on the first, third, fifth, seventh, and ninth following days (marked as +1d, +3d, +5d, +7d, +9d). It can be seen that the concentrations of nutrient salts evidently increased in the estuary area of the Shenzhen River while they remained unchanged in other areas of the bay on the first day after the storm; with the nutrient salts gradually being diffused into the bay under the effect of water exchange between the inside and outside of the bay (and there was no rainfall during these days), their concentrations decreased in the estuary area while they increased in the middle and outer parts of the bay; and with the water mass with high concentrations of nutrient salts moving towards the outer part of the bay and gradually being diffused, the nutrient salts' concentrations decreased in the inner part of the bay while they increased in the middle and outer parts during the fifth to seventh days after the storm event. Meanwhile, the distribution of the nutrient salts' concentrations in the various parts of the bay gradually became homogeneous, and on the ninth day after the rainfall, the distribution of nutrient salts' concentrations was similar to the values measured before the rainfall.

In addition, it is seen that the concentrations of NO_3-N and NH_3-N in the inner bay (especially in the estuary area of Shenzhen River) on the first day following the storm event (Figure 6(b1) and 6(b2)) were approximately as high as they were within the same range as the concentration values in Figure 2. Moreover, the concentrations of PO_4^{3-} (Figure 6(b3)) were obviously higher than the concentration values monitored in the water samples collected from the three kinds of pavements (Figure 2(a3), 2(b3), and 2(c3)). This was mainly due to: (1) the land-use types of the upstream and left bank of Shenzhen River being vegetation and water bodies (farmland, grassplots, and fishponds), which output large amounts of nutrient salts into the river and coastal waters in storms; and (2) the storm and flood

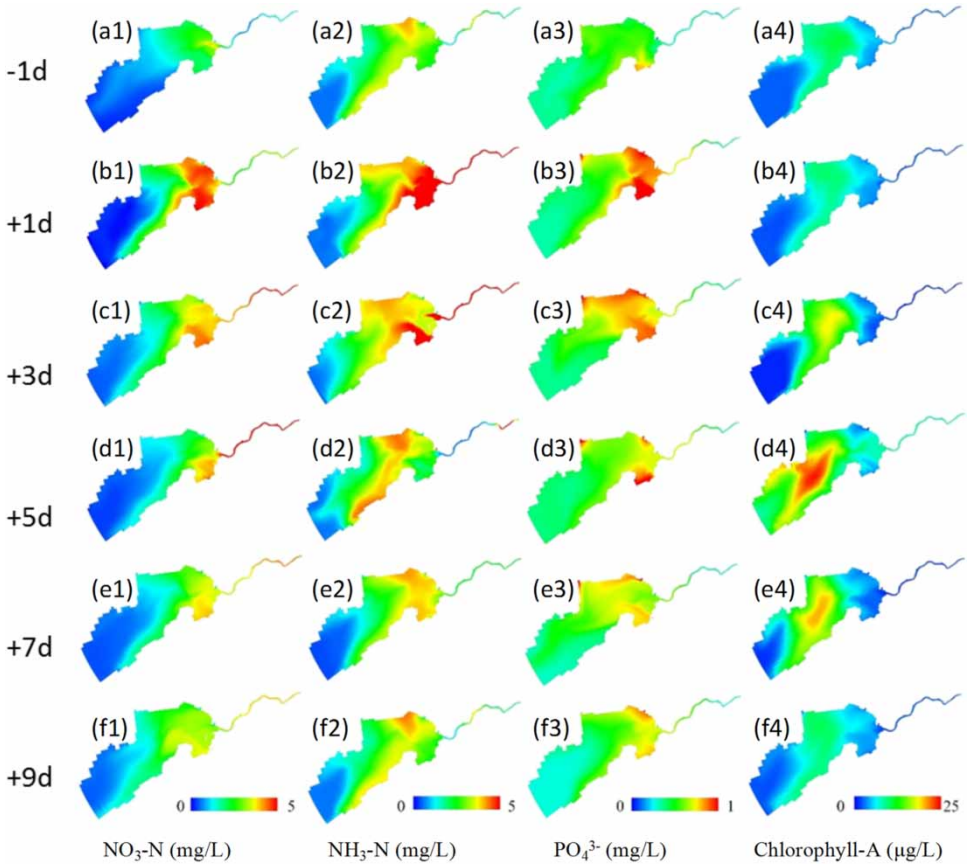

Figure 6 | The distribution of the monitored nutrient salts and chlorophyll-A in Shenzhen Bay after a storm event.

changed the hydro-dynamic conditions of the rivers and the bay, consequently, the polluted bottom mud released large amounts of N and P into the waterbody. As well, Figure 6(b3), to some extent, indicates that the paved surfaces were not the main source of PO_4^{3-} as its biogeochemical cycle has no significant atmospheric component.

In the case of the concentration of chlorophyll-A, due to the fact that a large amount of flood volume diluted the seawater near the estuary of the river, it evidently decreased during the first day after the storm event, while in other parts of the bay, the chlorophyll-A concentration remained unchanged. By the third day after the storm event, the tide and the diffusion of the nutrient salts resulted in the concentration of chlorophyll-A being gradually reversed to its normal levels in the estuary area of the bay. Due to the movement of the seawater, the nutrient salts migrated into the inner and middle parts of the bay; consequently, the chlorophyll-A concentration was raised in the inner and middle parts of the bay, while it remained unchanged in the outer part of the bay on the third day after the rainfall. On the fifth to seventh days after the rainfall, due to the accumulation of nutrient salts and the suitable weather conditions, the algae bloomed in the bay and the chlorophyll-A concentration achieved its peak value on the fifth day after the storm event. On the ninth day after the storm event, the chlorophyll-A concentration recovered to its normal levels, similar to that measured before the rainfall event.

In general, the inner part of the bay was significantly affected by the nutrient salts brought about by storm runoff soon after the storm event, and the middle part of the bay was only slightly affected by storm runoff pollutants. Meanwhile, the storm runoff pollutants had no influence on the water quality of the outer part of the bay. The variation of the distribution of chlorophyll-A concentration in Shenzhen Bay suggested an entirely different phenomenon taking place. The chlorophyll-A concentration in the middle part of

the bay was evidently higher than that in the other parts of the bay, and its peak appeared 5 days after the rainfall event occurred.

Impact of rainfall on bay eutrophication, modeled by EFDC under the designed rainfall

The designed rainfall events and the output of SWMM were used in EFDC to model the variation of the nutrient salts and chlorophyll-A concentrations in the bay. The analysis took into account the peak values of nutrient salts and chlorophyll-A concentration in different parts of the bay (evaluated at points A1, A2, and A3 in Figure 1) before and after the simulated rainfall event (indicated as CA_{PB} and CA_{PA}, respectively). Point A1 is located in the estuary, point A2 in the middle part of the bay, and point A3 in the mouth of the bay. The time between the start of the rainfall event and the moment when the peak values of chlorophyll-A concentration accrued is indicated as T1 and the time between the peak values of chlorophyll-A concentration and its recovery to normal levels as T2.

Tables 6–9 show the variation of CA_{PB}, CA_{PA}, T1, and T2, as modeled by EFDC under the designed storm events with different return periods. The simulation results indicate that the nutrient salts' concentrations in the estuary area (represented by point A1, Figure 1) increase rapidly and achieve peak values in about 6 hours after rainfall. The peak nutrient salts' concentrations increase with the

Table 6 | The variation of NH_3-N concentration before and after designed storm events in Shenzhen Bay

Return period (year)	CA_{PB} (mg/L)	CA_{PA} (mg/L)	T_1 (hours)	T_2 (hours)
T = 0.1	3.01/1.12/0.59[a]	3.31/1.20/0.60	6.5/72/–	89/72/–
T = 0.25	3.01/1.12/0.59	3.55/1.38/0.60	6.1/72/–	91/72/–
T = 0.5	3.01/1.12/0.59	3.79/1.48/0.62	5.9/71/–	93/73/–
T = 1	3.01/1.12/0.59	4.01/1.59/0.63	5.8/70/–	95/73/–
T = 2	3.01/1.12/0.59	4.25/1.62/0.61	5.7/68/–	95/74/–

[a]3.01/1.12/0.59 represents the concentration in estuary area/middle part/outer part of the bay.

Table 7 | The variation of NO_3-N concentration before and after designed storm events in Shenzhen Bay

Return period (year)	CA_{PB} (mg/L)	CA_{PA} (mg/L)	T_1 (hours)	T_2 (hours)
T = 0.1	3.24/1.15/0.85	3.45/1.26/0.87	6.4/71/–	93/72/–
T = 0.25	3.24/1.15/0.85	3.69/1.46/0.84	6.2/70/–	93/71/–
T = 0.5	3.24/1.15/0.85	3.85/1.55/0.83	6.0/72/–	96/73/–
T = 1	3.24/1.15/0.85	4.14/1.68/0.87	5.8/71/–	98/74/–
T = 2	3.24/1.15/0.85	4.32/1.73/0.85	5.7/69/–	99/74/–

Table 8 | The variation of PO_4^{3-} concentration before and after designed storm events in Shenzhen Bay

Return period (year)	CA_{PB} (mg/L)	CA_{PA} (mg/L)	T_1 (hours)	T_2 (hours)
T = 0.1	0.48/0.16/0.09	0.69/0.16/0.1	6.0/72/–	92/69/–
T = 0.25	0.48/0.16/0.09	0.81/0.17/0.1	6.0/71/–	94/71/–
T = 0.5	0.48/0.16/0.09	0.91/0.19/0.1	5.9/70/–	95/72/–
T = 1	0.48/0.16/0.09	0.98/0.2/0.1	6.0/70/–	97/72/–
T = 2	0.48/0.16/0.09	1.06/0.21/0.1	5.8/69/–	97/74/–

Table 9 | The variation of chlorophyll-A concentration before and after designed storm events in Shenzhen Bay

Return period (year)	CA_{PB} (μg/L)	CA_{PA} (μg/L)	T_1 (hours)	T_2 (hours)
T = 0.1	7.8/10.2/8.1	6.2/20.9/8.9	8.1/123/–	20/39/–
T = 0.25	7.8/10.2/8.1	6.5/22.6/8.0	8.2/118/–	20/39/–
T = 0.5	7.8/10.2/8.1	6.3/24.7/8.0	8.1/118/–	21/43/–
T = 1	7.8/10.2/8.1	6.2/27.9/7.9	8.8/115/–	23/45/–
T = 2	7.8/10.2/8.1	6.8/28.2/8.3	8.1/114/–	25/45/–

increase of rain volume, where the concentrations of NH_3-N, NO_3-N, and PO_4^{3-} increase from 3.31, 3.45, and 0.69 mg/L to 4.25, 4.32, and 1.06 mg/L, respectively. In approximately 4 days (89–99 hours) after the peak nutrient salts' concentration values appeared, the concentrations returned to their normal levels, similar to the peak values before rainfall. This phenomenon indicates that the storm runoff pollution continuously influences the nutrient salts' concentrations for 4–5 days.

In the middle part of the bay (represented by point A2, Figure 1), the nutrient salts' concentrations gradually increased and achieved peak values within about 3 days (68–72 hours) after the rainfall. The concentrations of NH_3-N, NO_3-N, and PO_4^{3-} increased from 1.2, 1.26, and 0.16 mg/L to 1.62, 1.73, and 0.21 mg/L, respectively. In approximately 3 days (69–74 hours) after the peak nutrient salts' concentration values appeared, the nutrient salts' concentrations returned to their normal levels, similar to the values before rainfall. However, the simulation results indicated that the storm runoff pollution essentially has no impact on the nutrient salts' concentrations in the outer part of Shenzhen Bay (represented by point A3, Figure 1).

In the case of the modeled chlorophyll-A, the concentration in the estuary area continuously decreased and reached its lowest values in about 8 hours due to the flood continuously flowing into the river mouth, diffusing the concentration of chlorophyll-A. Afterwards, the concentration of chlorophyll-A returned to its normal levels (similar to the concentration before rainfall) in about 1 day after the lowest value appeared. In the middle part of the bay, the chlorophyll-A concentration remained unchanged during about 3 days after the rainfall, subsequently increased on the fourth day after the rainfall and achieved its peak on the fifth day (114–123 hours) after the rainfall event. Meanwhile, the peak concentration values increased from 20.9 mg/L to 28.2 mg/L with the increase of the volume of rain in comparison with the peak concentration of 10.2 mg/L before rainfall. Nonetheless, the chlorophyll-A concentration in the outer part of the bay remained essentially the same.

In general, the modeled results from EFDC indicated that the storm runoff pollution influenced the water quality in the inner and middle parts of the bay obviously, but had essentially no impact on the water quality in the outer part of the bay. Furthermore, the variation of the nutrient salts' concentrations directly affected the variation of the chlorophyll-A concentration.

CONCLUSIONS

This study investigated the impacts of storm runoff pollution on eutrophication in Shenzhen Bay using monitored data and environmental models. The variation of the seawater quality was sensitive to the pollutants migrating as a result of the storm runoff. The following can be concluded:

1. EFDC driven by the output of SWMM (i.e., the pollutant loads in storm runoff) can satisfactorily model the variation of nutrient salts and chlorophyll-A concentrations in Shenzhen Bay.
2. Under the simulated storm events with the return periods varying from 0.5 to 2 years, the pollutant loads (NO_3-N, NH_3-N, and PO_4^{3-}) in storm runoff accounted for approximately 60–80% of the total pollutant loads in the urban area of the basin, and were significantly higher than the pollution produced by point-sources.
3. After the pollutant load migrated into Shenzhen Bay, the time lag between the pollutant loads generated from runoff and the algal bloom can be observed: the diffusion

of pollutants by hydrodynamic forces took a certain period of time and the nutrient salts absorbed by algae also took a certain period of time.

4. The storm runoff pollution mainly affected the seawater quality and eutrophication in the estuary area and the inner part of the bay, while the outer part of the bay was essentially free from the influence of pollution by storm runoff.

ACKNOWLEDGEMENTS

This research was supported by the Project of Technology & Innovation Commission of Shenzhen Municipality (ZDSYS20140509094114169). Hongliang Xu and Ying Zhang are co-first authors of the article.

REFERENCES

Bergman, M. J., Green, W. & Donnangelo, L. J. 2002 Calibration of storm loads in the South Prong watershed, Florida, using basins/HSPF 1. *Journal of the American Water Resources Association* **38** (5), 1423–1436.

Bertrand-Krajewski, J. L., Chebbo, G. & Saget, A. 1998 Distribution of pollutant mass vs volume in stormwater discharges and the first flush phenomenon. *Water Research* **32** (8), 2341–2356.

Bowes, M. J., House, W. A., Hodgkinson, R. A. & Leach, D. V. 2005 Phosphorus-discharge hysteresis during storm events along a river catchment: the River Swale, UK. *Water Research* **39** (5), 751–762.

Bricker, S. B., Longstaff, B., Dennison, W. C., Jones, A. B. & Woerner, J. L. 2008 Effects of nutrient enrichment in the nation's estuaries: a decade of change. *Harmful Algae* **8** (1), 21–32.

Brinkmann, W. L. F. 1985 Urban stormwater pollutants: sources and loadings. *GeoJournal* **11** (3), 277–283.

Burian, S. J., Streit, G. E., McPherson, T. N., Brown, M. J. & Turin, H. J. 2001 Modeling the atmospheric deposition and stormwater washoff of nitrogen compounds. *Environmental Modelling & Software* **16** (5), 467–479.

Carpenter, S. R., Caraco, N. F., Correll, D. L., Howarth, R. W., Sharpley, A. N. & Smith, V. H. 1998 Nonpoint pollution of surface waters with phosphorus and nitrogen. *Ecological Applications* **8** (3), 559–568.

Chang, T. J., Wang, C. H. & Chen, A. S. 2015 A novel approach to model dynamic flow interactions between storm sewer system and overland surface for different land covers in urban areas. *Journal of Hydrology* **524**, 662–679.

Chen, L., Yang, Z. & Liu, H. 2016 Assessing the eutrophication risk of the Danjiangkou Reservoir based on the EFDC model. *Ecological Engineering* **96**, 117–127.

Chen, Y., Cebrian, J., Lehrter, J., Christiaen, B., Stutes, J. & Goff, J. 2017 Storms do not alter long-term watershed development influences on coastal water quality. *Marine Pollution Bulletin* **122** (1–2), 207–216.

Conley, D. J., Paerl, H. W., Howarth, R. W., Boesch, D. F., Seitzinger, S. P., Havens, K. E., Lancelot, C. & Likens, G. E. 2009 Controlling eutrophication: nitrogen and phosphorus. *Science* **323** (5917), 1014–1015.

Dai, W., Gao, J., Cao, G. & Ouyang, F. 2013 Chemical composition and source identification of PM 2.5, in the suburb of Shenzhen, China. *Atmospheric Research* **122** (3), 391–400.

EFDC User Manual 2007 US EPA, Tetra Tech, Fairfax, VA, USA.

Estalaki, S. M., Kerachian, R. & Nikoo, M. R. 2016 Developing water quality management policies for the Chitgar urban lake: application of fuzzy social choice and evidential reasoning methods. *Environmental Earth Sciences* **75** (5), 1–16.

Gnecco, I., Berretta, C., Lanza, L. G. & Barbera, P. L. 2005 Storm water pollution in the urban environment of Genoa, Italy. *Atmospheric Research* **77** (1), 60–73.

Goonetilleke, A., Thomas, E., Ginn, S. & Gilbert, D. 2005 Understanding the role of land use in urban stormwater quality management. *Journal of Environmental Management* **74** (1), 31–42.

Guan, M., Sillanpää, N. & Koivusalo, H. 2015 Storm runoff response to rainfall pattern, magnitude and urbanization in a developing urban catchment. *Hydrological Processes* **30** (4), 543–557.

Hamrick, J. M. & Wu, T. S. 1997 *Computational Design and Optimization of the EFDC/HEM3D Surface Water Hydrodynamic and Eutrophication Models*. Society for Industrial and Applied Mathematics, Philadelphia, PA, USA, pp. 143–161.

Hathaway, J. M., Tucker, R. S., Spooner, J. M. & Hunt, W. F. 2012 A traditional analysis of the first flush effect for nutrients in stormwater runoff from two small urban catchments. *Water, Air, & Soil Pollution* **223** (9), 5903–5915.

Johnson, R. D. & Sample, D. J. 2017 A semi-distributed model for locating stormwater best management practices in coastal environments. *Environmental Modelling & Software* **91**, 70–86.

Josefson, A. B. & Rasmussen, B. 2000 Nutrient retention by benthic macrofaunal biomass of Danish estuaries: importance of nutrient load and residence time. *Estuarine, Coastal and Shelf Science* **50** (2), 205–216.

Kemp, W. M., Boynton, W. R., Adolf, J. E., Boesch, D. F., Boicourt, W. C., Brush, G., Cornwell, J. C., Fisher, T. R., Glibert, P. M., Hagy, J. D., Harding, L. W., Houde, E. D., Kimmel, D. G., Miller, W. D., Newell, R. I. E., Roman, M. R., Smith, E. M. & Stevenson, J. C. 2005 Eutrophication of Chesapeake Bay: historical trends and ecological interactions. *Marine Ecology Progress Series* **303** (21), 1–29.

Lessin, G. & Raudsepp, U. 2007 Modelling the spatial distribution of phytoplankton and inorganic nitrogen in Narva Bay, southeastern Gulf of Finland, in the biologically active period. *Ecological Modelling* **201** (3–4), 348–358.

Liu, Z., Hashim, N. B., Kingery, W. L., Huddleston, D. H. & Xia, M. 2008 Hydrodynamic modeling of St. Louis Bay estuary and watershed using EFDC and HSPF. *Journal of Coastal Research* **52** (Fall 2008), 107–116.

Machado, D. A. & Imberger, J. 2014 Modeling the impact of natural and anthropogenic nutrient sources on phytoplankton dynamics in a shallow coastal domain, Western Australia. *Environmental Fluid Mechanics* **14** (1), 87–111.

Maillard, P. & Santos, N. A. P. 2008 A spatial-statistical approach for modeling the effect of non-point source pollution on different water quality parameters in the Velhas river watershed–Brazil. *Journal of Environmental Management* **86** (1), 158–170.

O'Donncha, F., Ragnoli, E. & Suits, F. 2013 Parallelisation study of a three-dimensional environmental flow model. *Computers & Geosciences* **64** (C), 96–103.

Park, K., Jung, H. S., Kim, H. S. & Ahn, S. M. 2005 Three-dimensional hydrodynamic-eutrophication model (HEM-3D): application to Kwang-Yang Bay, Korea. *Marine Environmental Research* **60** (2), 171–193.

Rossi, L., Calizza, E., Careddu, G., Rossi, D., Orlandi, L., Jona-Lasinio, G., Aguzzi, L. & Costantini, M. L. 2018 Space-time monitoring of coastal pollution in the Gulf of Gaeta, Italy, using δ^{15}n values of, Ulva lactuca, landscape hydromorphology, and Bayesian Kriging modelling. *Marine Pollution Bulletin* **126**, 479–487.

Saniewska, D., Bełdowska, M., Bełdowski, J., Saniewski, M., Gębka, K., Szubska, M. & Wochna, A. 2018 Impact of intense rains and flooding on mercury riverine input to the coastal zone. *Marine Pollution Bulletin* **127**, 593–602.

Seinfeld, J. H., Pandis, S. N. & Noone, K. 1998 *Atmospheric Chemistry and Physics: From Air Pollution to Climate Change*. Wiley, Chichester, UK.

Shuster, W. D., Dadio, S. D., Burkman, C. E., Earl, S. R. & Hall, S. J. 2015 Hydropedological assessments of parcel-level infiltration in an arid urban ecosystem. *Soil Science Society of America Journal* **79** (2), 398.

Temprano, J., Arango, Ó., Cagiao, J., Suárez, J. & Tejero, I. 2006 Stormwater quality calibration by SWMM: a case study in Northern Spain. *Water SA* **32** (1), 55–63.

Turner, R. E. & Rabalais, N. N. 2004 Suspended sediment, C, N, P, and Si yields from the Mississippi River Basin. *Hydrobiologia* **511** (1–3), 79–89.

Villarino, M. L., Figueiras, F. G., Jones, K. J., Alvarez-Salgado, X. A. & Edwards, A. 1995 Evidence of in situ diel vertical migration of a red-tide microplankton species in Ria de Vigo (NW Spain). *Marine Biology* **123** (3), 607–617.

Wool, T. A., Davie, S. R. & Rodriguez, H. N. 2003 Development of three-dimensional hydrodynamic and water quality models to support total maximum daily load decision process for the Neuse River Estuary, North Carolina. *Journal of Water Resources Planning and Management* **129** (4), 295–306.

First received 27 January 2019; accepted in revised form 23 April 2019. Available online 20 May 2019